Copy No. 45
RM No. SL9E13

NACA

RESEARCH MEMORANDUM

for the

Air Materiel Command, U. S. Air Force

A PRELIMINARY ANALYSIS OF THE FLYING QUALITIES OF THE CONSOLIDATED VULTEE MX-813 DELTA-WING AIRPLANE CONFIGURATION AT TRANSONIC AND LOW SUPERSONIC SPEEDS AS DETERMINED FROM FLIGHTS OF ROCKET-POWERED MODELS

By

Grady L. Mitcham

Langley Aeronautical Laboratory
Langley Air Force Base, Va.

NATIONAL ADVISORY COMMITTEE
FOR AERONAUTICS

WASHINGTON

1949

NACA RM No. SL9E13

NATIONAL ADVISORY COMMITTEE FOR AERONAUTICS

RESEARCH MEMORANDUM

for the

Air Materiel Command, U. S. Air Force

A PRELIMINARY ANALYSIS OF THE FLYING QUALITIES OF THE CONSOLIDATED VULTEE MX-813 DELTA-WING AIRPLANE CONFIGURATION AT TRANSONIC AND LOW SUPERSONIC SPEEDS AS DETERMINED FROM FLIGHTS OF ROCKET-POWERED MODELS

By Grady L. Mitcham

SUMMARY

A preliminary analysis of the flying qualities of the Consolidated Vultee MX-813 delta-wing airplane configuration has been made based on the results obtained from the first two $\frac{1}{8}$-scale models flown at the NACA Pilotless Aircraft Research Station, Wallops Island, Va. The Mach number range covered in the tests was from 0.9 to 1.2.

The analysis indicates adequate elevator control for trim in level flight over the speed range investigated. Through the transonic range there is a mild trim change with a slight tucking-under tendency. The elevator control effectiveness in the supersonic range is reduced to about one-half the subsonic value although sufficient control for maneuvering is available as indicated by the fact that 10° elevator deflection produced 5g acceleration at a Mach number of 1.2 at 40,000 feet. The elevator control forces are high and indicate the power required of the boost system. The damping of the short-period oscillation is adequate at sea level but is reduced at 40,000 feet. The directional stability appears adequate for the speed range and angles of attack covered.

INTRODUCTION

At the request of the Air Materiel Command, U. S. Air Force, flight tests of $\frac{1}{8}$-scale rocket-powered models of the Consolidated Vultee MX-813 are being made to evaluate the drag and longitudinal stability and

control characteristics at transonic and low supersonic speeds at the NACA Pilotless Aircraft Research Station, Wallops Island, Va. A total of six models, four of which have been flown, were supplied for the investigation. The first model was lost due to a structural failure. Three models which were instrumented for a study of longitudinal stability and control have been flown successfully. The present paper is preliminary in that it is based on only the first two of the three successful models flown and does not represent a complete analysis. These two models are referred to herein as model 1 and model 2.

The MX-813 tailless airplane has a wing of triangular plan form with 60° sweepback of the leading edge and an aspect ratio of 2.31; the profile at all spanwise stations is an NACA 65(06)-006.5 section. Longitudinal and lateral control are provided by a single set of constant-chord trailing-edge control surfaces on the wing called elevons. Deflecting the elevons together provides longitudinal control and deflecting them differentially gives lateral control. The vertical tail is of triangular plan form with a leading-edge sweepback of 60°.

A flying mock-up of the MX-813, designated as the Consolidated Vultee 7002, was designed by the contractor, and flight tests of the 7002 configuration at transonic speeds are contemplated. The fuselage of this configuration is somewhat smaller and of a different shape than that of the MX-813. The fuselage nose sections on the $\frac{1}{8}$-scale models, which otherwise represented the MX-813 configuration, were modified to approximate the existing nose on the 7002 configuration with the exception of the air intake on the airplane which was faired to a cone on the model. A comparison of the full-scale 7002 airplane and the $\frac{1}{8}$-scale MX-813 model is presented in figure 1.

The models were flown with a programmed-type control which called for abrupt pull-ups and push-downs with the elevons operated as elevators. The flight test for model 1 was conducted on September 11, 1948 and for model 2 on October 15, 1948.

This paper contains the important sections of the flight time histories and the results of an analysis of the high-speed flying qualities to be expected from the MX-813 in the Mach number range from 0.9 to 1.2 based on the results obtained from the flight tests. The analysis is presented for the full-scale configuration with a wing loading of 27.3 pounds per square foot at sea level and at an altitude of 40,000 feet. The computations are based on two center-of-gravity positions, 20 percent and 25 percent of the mean aerodynamic chord. An analysis of the data in terms of aerodynamic coefficients and stability derivatives is in progress for all three stability models flown.

SYMBOLS

t	time from launching, seconds
M	Mach number
V_c	velocity of sound, feet per second
p	free-stream static pressure, pounds per square foot
γ	specific heat ratio; value taken, 1.40
H	hinge moment, inch-pounds; total-head pressure (equations (1) and (2)), pounds per square foot
$\bar{c}$	mean aerodynamic chord, feet
a_l	longitudinal acceleration, feet per second per second
a_n	normal acceleration, feet per second per second
a_t	transverse acceleration, feet per second per second
g	acceleration due to gravity, 32.2 feet per second per second
δ_e	control deflection measured on chord line parallel to the plane of symmetry, degrees
α	angle of attack measured from fuselage center line, degrees
R	Reynolds number $\left(\frac{\rho V \bar{c}}{\mu}\right)$
W	weight, pounds
S	wing area, square feet
q	free-stream dynamic pressure, pounds per square foot $\left(\frac{\rho V^2}{2}\right)$
ρ	mass density of air, slugs per cubic foot
C_c	chord-force coefficient $\left(\frac{a_l}{g}\frac{W}{S}\frac{1}{q}\right)$

C_N	normal-force coefficient $\left(\frac{a_n}{g}\frac{W}{S}\frac{1}{q}\right)$
C_L	lift coefficient ($C_N \cos \alpha + C_c \sin \alpha$)
$C_{L_{trim}}$	trim lift coefficient
C_{L_α}	rate of change of lift coefficient with angle of attack, per degree
$C_{L_{\delta_{trim}}}$	rate of change of trim lift coefficient with elevator deflection, per degree
$\delta_{e_{trim}}$	trim control deflection, degrees
x	stick movement, inches
F	stick force, pounds
P	period of an oscillation, seconds
I_Y	moment of inertia about pitch axis, slug-feet^2
$C_{m_{\frac{\dot{\theta}\bar{c}}{2V}}} + C_{m_{\frac{\dot{\alpha}\bar{c}}{2V}}}$	total damping factor
$\Delta T_{1/2}$	time to damp to 1/2 amplitude, seconds
m	mass, slugs
Subscripts:	
a	full-scale airplane
m	model

MODELS AND APPARATUS

Models

A three-view drawing of the $\frac{1}{8}$-scale model used in the present investigation is given in figure 1. The physical characteristics of the full-scale Consolidated Vultee 7002 airplane and of the $\frac{1}{8}$-scale models of the MX-813 are presented in table I. Since the $\frac{1}{8}$-scale

models were designed, with modifications of fuselage nose sections, from the original MX-813 configuration, the values are not exactly one-eighth of the values of the full-scale 7002 configuration. Photographs of one of the MX-813 models are shown as figures 2 and 3. The model fuselage and components were constructed of duralumin, magnesium castings, and magnesium skin. The fuselage construction was of the monocoque type and was divided into three sections. The three sections were the nose section, which held the telemeter; the center section which held the wings, tail, compressed-air supply, and control-actuating system; and the tail section which contained the rocket sustainer motor and booster attachment.

The programmed movement of the elevons was accomplished by a compressed-air system which called for abrupt pull-ups and push-downs at a frequency of about one cycle per 1.2 seconds. The control surfaces, which were unsealed, moved together between stops in a square-wave motion. On model 1 the surfaces were deflected down 5.3° and up 5.3°; on model 2 the deflection was down 4.7° and up 4.7°. This control motion was in operation during the entire flight. Prior to each flight the control system was subjected to a static load test at two locations along the span of the elevon to determine the twist that would be encountered along the span and in the control-linkage system under high aerodynamic loads. The elevator-deflection data presented in this paper were corrected on the basis of these tests.

The models were boosted to supersonic speeds by a dry-fuel, 6-inch-diameter Deacon rocket motor, which is capable of producing an average thrust of 6500 pounds for approximately 3.1 seconds.

The rocket sustainer motor for the model was a 5-inch HVAR dry-fuel rocket shortened to 17 inches and modified to give an average thrust of 900 pounds for 1.4 seconds. The small sustainer motor served a two-fold purpose: during the power-on portion of the flight, the motor allowed the controls to operate one complete cycle at approximately a constant Mach number and assured a positive separation between model and booster at booster burnout.

The sustainer-motor nozzle served as the point of attachment of the booster to the model. This type of attachment allowed a drag separation of the booster from the model at cessation of booster thrust inasmuch as the drag-weight ratio of the model was less than the drag-weight ratio of the booster.

The booster-model combinations were ground-launched from a crutch-type launcher. (See fig. 4.) The launching angle for model 1 was 43° 40' from the horizontal and for model 2 was 44° 40'. Table II presents the weight and balance data for the models and for the full-scale airplane. Figure 5 shows a sequence of photographs of the booster-model combination at take-off.

Apparatus

The data from the flights were obtained by the use of telemeters, Doppler velocimeter radar unit, photography, and radiosonde. The time histories of the data as the models traversed the Mach number range were transmitted and recorded by a telemeter system which gave eight channels of information: four channels of continuous signal and four channels of intermittent signal. The data recorded were longitudinal, transverse, and normal acceleration; hinge moment; control position; angle of attack; total head; and a calibrated static pressure used to determine free-stream static pressure. Angles of attack were obtained by a vane-type angle-of-attack indicator located on a sting ahead of the nose of the model. The pressures obtained from the telemeter records were reduced to Mach number by the following equations:

Subsonic

$$\frac{H}{p} = \left(1 + \frac{\gamma - 1}{2} M^2\right)^{\frac{\gamma}{\gamma-1}} \tag{1}$$

Supersonic

$$\frac{H}{p} = \frac{\left(\frac{\gamma + 1}{2} M^2\right)^{\frac{\gamma}{\gamma-1}}}{\left(\frac{2\gamma}{\gamma + 1} M^2 - \frac{\gamma - 1}{\gamma + 1}\right)^{\frac{1}{\gamma-1}}} \tag{2}$$

where p was obtained from the calibrated static-pressure data. The maximum altitude attained on model 1 was approximately 4000 feet, while on model 2 the maximum altitude reached was 4700 feet. The Doppler velocimeter radar unit served as an independent check of the Mach number obtained by use of the total and static pressures.

Fixed wide-angle cameras and 16-millimeter motion-picture cameras recorded the launchings, and the flights were tracked by 16-millimeter color motion-picture cameras.

TEST TECHNIQUE

The model was disturbed in pitch by abrupt movement of elevons operated as elevators at preset time intervals which gave a square-wave-type elevator motion. The flying qualities of the full-scale airplane were calculated from an analysis of the forces and motions resulting from these cyclic disturbances.

[redacted]

BASIS OF ANALYSIS

The most recent specifications for satisfactory flying qualities (references 1 and 2) have been used as a guide in the present analysis. However, inasmuch as the analysis is restricted to the behavior of the model at transonic speeds, no detailed step-by-step comparison with these specifications has been attempted.

The Reynolds number and Mach number ranges for the full-scale MX-813 airplane and the $\frac{1}{8}$-scale models are presented in figure 6.

An evaluation of the effect of damping in pitch on the control position required for trim indicated the effect to be of small magnitude with the maximum effect being 1.5 percent at sea level and 3 percent at 40,000 feet for a Mach number of 0.91. This error decreased with increasing Mach number because of a decrease in elevator effectiveness at transonic and low supersonic speeds. The data presented are not corrected for this effect.

The flying qualities were estimated from the actual time histories of flight models 1 and 2. The method and steps necessary to reduce the flight records to flying qualities are described in detail.

Variation with Mach Number of the Control Position Required for Trim in Level Flight

The trim lift coefficient $C_{L_{trim}}$ for 0° elevator deflection was obtained by plotting values of C_L corresponding to constant positive and negative elevator deflections against Mach number. These values were taken from the trim values of C_L and δ_e obtained from the time-history data of the flight test of the two $\frac{1}{8}$-scale models. Figure 7 presents a typical section of a time history and the method of determining trim values from the oscillations. The value of $C_{L_{trim}}$ for $\delta_e = 0°$ was obtained by interpolation. Values of C_L for level flight for the full-scale airplane were obtained from the relation $C_{L(1\ g)} = \frac{W/S}{q}$. The difference between $C_{L(1\ g)}$ for straight and level

flight and $C_{L_{trim}}$ for $\delta_e = 0^\circ$ was divided by $C_{L_{\delta_{trim}}}$ to give δ_e for straight and level flight for various Mach numbers:

$$\delta_e = \frac{C_{L(1\ g)} - C_{L_{trim(\delta=0^\circ)}}}{C_{L_{\delta_{trim}}}}$$

Elevator Control Force for Trim against Mach Number

A value of deflection of elevator per inch of stick movement for a high-speed fighter-type airplane was assumed to be

$$\frac{\delta_e}{x} = 2 \text{ degrees per inch}$$

Values of hinge moment were obtained from the time-history plots of the $\frac{1}{8}$-scale flight-test models for corresponding $\delta_{e_{trim}}$ values against Mach number. The method for determining trim lines was the same as in figure 7. The value of $\left(\frac{\Delta H}{\Delta \delta_e}\right)_{trim}$ was obtained from

$$\left(\frac{\Delta H}{\Delta \delta_e}\right)_{trim} = \frac{\left(H_2 - H_1\right)_{trim}}{\left(\delta_{e_2} - \delta_{e_1}\right)_{trim}}$$

At a given Mach number a value of hinge moment was read at a given elevator deflection and corrected to the $\delta_{e_{trim}}$ for straight and level flight sea-level conditions by

$$H\delta_{e_{trim}} = H_1 - \left[\left(\delta_{e_1} - \delta_{e_{trim}}\right)\left(\frac{\Delta H}{\Delta \delta_e}\right)_{trim}\right]$$

If the hinge moment for $\delta_{e_{trim}}$ for straight and level flight at sea-level conditions is known, the elevator-control force is obtained by

CONFIDENTIAL

$$F = \frac{H}{57.3} \frac{\delta_e}{x}$$

where H has been corrected to full scale.

Change in Normal Acceleration for a Corresponding Change in Elevator Deflection $\frac{\Delta g}{\Delta \delta_e}$ against Mach Number

The values of C_L for level flight for various Mach numbers were divided by $C_{L_{\delta_{trim}}}$ so that

$$\Delta \delta_e = \frac{C_{L(1\ g)}}{C_{L_{\delta_{trim}}}}$$

for 1 g. The reciprocal of this quantity is the required quantity

$$\frac{\Delta g}{\Delta \delta_e} = \frac{1}{\left(\frac{\Delta \delta_e}{1\ g}\right)}$$

Change in Trim Angle of Attack for a Corresponding Change in Trim Elevator Deflection $\left(\frac{\Delta \alpha}{\Delta \delta_e}\right)_{trim}$ as a Function of Mach Number

The change in trim angle of attack was divided by the corresponding change in trim elevator deflection at constant Mach numbers:

$$\left(\frac{\Delta \alpha}{\Delta \delta_e}\right)_{trim} = \frac{\left(\alpha_2 - \alpha_1\right)_{trim}}{\left(\delta_{e_2} - \delta_{e_1}\right)_{trim}}$$

Stick Force per g against Mach Number

The change in elevator deflection required for a change in normal acceleration of 1 g, reciprocal of $\frac{\Delta g}{\Delta \delta_e}$, were multiplied by $\frac{\Delta H}{\Delta \delta_{e_{trim}}}$ to obtain the change in hinge moment required for a change in normal acceleration of 1 g. Then for $\frac{\Delta F}{g}$ in pounds per g:

$$\frac{\Delta F}{g} = \frac{\Delta \delta_e}{g} \frac{\Delta H}{\Delta \delta_{e_{trim}}} \frac{\delta_e}{x} \frac{1}{57.3}$$

Dynamic Stability

The dynamic stability of the airplane in terms of period and damping of the short-period longitudinal oscillation were determined from the oscillations of the model corrected to full-scale conditions. The correction factors were determined from a two-degree-of-freedom method of analysis of the motion which assumes no changes in forward speed during the oscillation. The period of the oscillation for the airplane in terms of period for the model is

$$P_a = P_m \frac{V_{c_m}}{V_{c_a}} \sqrt{\frac{I_{Y_a}}{S_a \bar{c}_a} \frac{S_m \bar{c}_m}{I_{Y_m}} \frac{\rho_m}{\rho_a}}$$

The rate of change of the pitching-moment coefficient with angle of attack is omitted from this equation since the center of gravity for the model and that for the airplane is the same. The time to damp to one-half amplitude for the airplane was determined by the following relationship:

$$C_{m_{\frac{\dot{\theta}\bar{c}}{2V}}} + C_{m_{\frac{\dot{\alpha}\bar{c}}{2V}}} = \frac{-8I_Y}{\rho V_c MS\bar{c}^2} \left(\frac{0.693}{\Delta T_{1/2}} - \frac{57.3 C_{L_\alpha} \rho V_c MS}{4m} \right)$$

and equated for model and airplane as follows:

$$\frac{0.693}{\Delta T_{1/2_a}} = \frac{-57.3 C_{L_\alpha} \rho_a V_{c_a} M S_a}{4} \left(-\frac{1}{m_a} + \frac{I_{Y_m} \bar{c}_a^2}{I_{Y_a} m_m \bar{c}_m^2} \right) + \frac{I_{Y_m} V_{c_a} \rho_a S_a \bar{c}_a^2}{I_{Y_a} V_{c_m} \rho_m S_m \bar{c}_m^2} \frac{0.693}{\Delta T_{1/2_m}}$$

RESULTS AND DISCUSSION

Time Histories

Time histories of the important parts of flight for models 1 and 2 are given in figures 8 and 9 and a plot of $\frac{W/S}{q}$ is given in figure 10. On model 1, longitudinal acceleration was a switched channel as shown in figure 8. The channel markers indicated in the angle-of-attack, control position, hinge moment, and normal-acceleration channels on figure 8 serve to identify the channels and during this time interval no values are recorded; the dashed lines are estimated from the shape of similar oscillations. The hinge-moment and transverse-acceleration channels were switched to give intermittent signals on model 2 as shown in figure 9. The short dashed lines were estimated from the results obtained on model 1. The solid portions of the curves are the actual data obtained from the flight. The elevator deflections as presented in figures 8 and 9 have been corrected for the twist in the system caused by the hinge moment; the angles of attack have been corrected for the difference in angle between the angle-of-attack vane and the center of gravity.

Longitudinal Trim Characteristics

The characteristics of the elevator control in level flight of the MX-813 configuration are presented in figure 11 in the form of the variation of the elevator position required for trim with Mach number. Control-position trim change is manifested between a Mach number of 0.90 and 0.96 at sea level and at 40,000 feet. The control-position trim change is a function of variation of out-of-trim pitching moment with Mach number, change in control effectiveness, and the movement of the neutral point. The resultant changes in trim, tucking-under tendency, appear to be relatively gradual and of moderate magnitude. For example, at 40,000 feet a maximum up elevator angle of about 5° is required at a Mach number of 0.96.

An evaluation of the stick-fixed maneuver point in the Mach number range between 0.90 and 1.2 indicated that the point is well behind the most rearward center-of-gravity position and the requirements are met for maneuvering stability in reference 1.

Longitudinal control forces.- The elevator-control force required for trim in straight and level flight at various Mach numbers is presented in figure 12 and the stick force per g is presented in figure 13. These stick forces are based on a conventional airplane configuration with 2° of elevator deflection to 1 inch of stick movement. This assumption was necessary since the full-scale MX-813 is provided with an irreversible 100-percent hydraulic boost control system; therefore, no relation exists between hinge moments and stick forces. The data do indicate, however, the power required of the control boost system with no balancing and trimming devices. For example, at a Mach number of 1.2 at 40,000 feet, the stick force per g based on measured hinge moments is about 1000 per g.

The variation of elevator-control force for trim with Mach number (fig. 12) indicated that pull forces were required at all speeds below the trim speed and push forces required at all speeds above the trim speed within the range of Mach numbers from 0.96 to 1.2. The opposite is true from Mach numbers of 0.9 to 0.96, but the elevator angle for trim in this range of Mach number increases with increasing Mach number. However, the stick force would be in the correct sense with respect to stick movement throughout the transonic region.

The elevator hinge-moment data obtained for model 1 indicate a force reversal at high angles of attack ($\alpha = 15°$) at Mach numbers below 0.9. Model 2, which flew at angles of attack of about 7° at M = 0.9, did not show a hinge-moment reversal but did indicate hinge moments near zero.

Longitudinal control effectiveness.- The variation with Mach number of the normal acceleration produced per unit elevator deflection $\frac{\Delta g}{\Delta \delta_e}$ is presented in figure 14. At sea level a large transition in elevator effectiveness was apparent from subsonic to low supersonic speeds with minimum effectiveness occurring at a Mach number of 1.06 for model 1 with the center-of-gravity location at 25-percent mean aerodynamic chord and at a Mach number of 0.98 for model 2 with the center-of-gravity location at 20-percent mean aerodynamic chord. Sufficient control for maneuvering is available as indicated by the fact that 10° elevator deflection produced 5g acceleration at a Mach number of 1.2 at 40,000 feet.

Another measure of control effectiveness is the angle-of-attack change produced per degree elevator deflection $\left(\frac{\Delta\alpha}{\Delta\delta_e}\right)_{trim}$ (fig. 15). The effectiveness of the elevator in changing angle of attack at supersonic speeds is reduced to about one-half of the subsonic value. This change of effectiveness occurs gradually. This effect was particularly noticeable on model 1 with the rearward center of gravity where the trim angles of attack below M = 0.9 were greater than the range of the angle-of-attack vane. The decrease in control effectiveness is evidence of the increased stability of the configuration and the decreased lift effectiveness of the trailing-edge flap that can be expected at supersonic speeds as compared with high subsonic speeds.

Dynamic stability.- The characteristics of the stick-fixed short-period longitudinal oscillations are presented in figures 16, 17, and 18. U. S. Air Force specifications for stability and control characteristics of airplanes require that the short-period dynamic oscillation of normal acceleration produced by moving and quickly releasing the elevator shall be damped to 1/10 amplitude in one cycle (based on free controls). The damping characteristics for the full-scale MX-813 have been evaluated for the control-fixed condition, although there is a slight oscillation in the control position due to hinge-moment effect, which is apparent in figures 7 and 8. The fixed-control characteristics will dictate the behavior of the MX-813 since it is equipped with an irreversible 100-percent hydraulic boost control system. Figures 17 and 18 indicate that this tailless design would more than meet such a requirement at sea level since the longitudinal short-period oscillation will damp to an average value of 1/16 amplitude in one cycle. At 40,000 feet, however, the damping is reduced to about 1/3 of the sea-level value.

Directional stability.- Model 2 apparently had some directional asymmetry causing it to develop a small positive side force throughout the flight. This effect became about twice as large at Mach numbers below 0.9. Model 1 did not exhibit any such consistent side-force variation, the side forces on model 1 resulting from an occasional disturbance. Neither model showed divergence or continuous oscillations thus indicating positive directional stability.

CONCLUSIONS

An analysis of the flying qualities of the MX-813, based on the results obtained from two $\frac{1}{8}$-scale models, for Mach numbers 0.9 to 1.2 indicates the following conclusions for the full-scale airplane:

1. There is ample elevator control for trim in level flight at sea level or at altitude. At 40,000 feet a maximum up elevator angle of about 5° is required at a Mach number of 0.96. The transonic trim change, a tucking-under tendency, appears to be mild.

2. The elevator control remains effective in changing lift or angle of attack over the entire speed range. The effectiveness of the elevator in changing angle of attack, however, is reduced to about half of its subsonic value at supersonic speeds. This change of effectiveness occurs gradually.

3. With the center of gravity at 25-percent mean aerodynamic chord the normal acceleration produced per degree elevator is such that about 10° up elevator are required to produce 5g at 40,000 feet at a Mach number of 1.2. The corresponding stick force per g based on the measured hinge moments is about 1000 pounds per g, a figure which gives an indication of the power required of the control boost system.

4. The damping of the short-period longitudinal oscillation is adequate over the speed range for the sea-level condition (of the order of 1 cycle to damp to 1/16 amplitude). At 40,000 feet, however, the damping is reduced to about 1/3 the sea-level value.

5. The directional stability appears to be adequate throughout the speed and angle-of-attack range investigated.

Langley Aeronautical Laboratory
National Advisory Committee for Aeronautics
Langley Air Force Base, Va.

Grady L. Mitcham
Grady L. Mitcham
Aeronautical Engineer

Approved:

Robert R. Gilruth
Robert R. Gilruth
Chief of Pilotless Aircraft Research Division

JMS

[redacted]

1. Anon.: Flying Qualities of Piloted Airplanes. U. S. Air Force Specification No. 1815-B, June 1, 1948.

2. Gilruth, R. R.: Requirements for Satisfactory Flying Qualities of Airplanes. NACA Rep. No. 755, 1943.

[redacted]

TABLE I

PHYSICAL CHARACTERISTICS OF THE FULL-SCALE CONSOLIDATED VULTEE 7002 AND THE $\frac{1}{8}$-SCALE MODELS 1 AND 2 OF THE MX-813 CONFIGURATION

	$\frac{1}{8}$-scale model (MX-813)	Full-scale configuration
Wing:		
Area, sq ft (included)	6.25	425
Span, ft	3.80	31.33
Aspect ratio	2.31	2.31
Mean aerodynamic chord, ft	2.19	18.08
Sweepback of leading edge, deg	60	60
Dihedral (relative to mean thickness line), deg	0	0
Taper ratio (Tip chord/Root chord)	0	0
Airfoil section	NACA 65-006.5	NACA 65-006
Vertical tail:		
Area (outside of fuselage), sq ft	0.81	76.0
Height (outside of fuselage), ft	0.97	9.31
Aspect ratio	1.16	1.14
Sweepback of leading edge, deg	60	60
Taper ratio (Tip chord/Root chord)	0	0
Airfoil section	NACA 65-006.5	NACA 65-006
Elevon:		
Type	Plain flap	----------
Area (aft of hinge line, one) sq ft	0.51	38.3
Span (at trailing edge of wing, one) ft	1.78	----------
Chord (hinge line to trailing edge), ft	0.37	----------

TABLE II

WEIGHT AND BALANCE DATA FOR $\frac{1}{8}$-SCALE MX-813 MODELS 1 AND 2 AND FULL-SCALE CONSOLIDATED VULTEE 7002 CONFIGURATION

Rocket fuel included on the $\frac{1}{8}$-scale models				
Model	Weight (lb)	Wing loading (lb/sq ft)	Center-of-gravity position (percent M.A.C.)	Moment of inertia, I_Y (slug-ft^2)
1	188.00	30.1	29.7	17.52
2	189.75	30.4	24.0	17.89
$\frac{1}{8}$-scale models without rocket fuel				
Model	Weight (lb)	Wing loading (lb/sq ft)	Center-of-gravity position (percent M.A.C.)	Moment of inertia, I_Y (slug-ft^2)
1	182.50	29.2	25.0	16.65
2	184.25	29.5	20.0	17.10
Full-scale 7002				
Normal gross weight (lb)		Wing loading (lb/sq ft)	Center-of-gravity position (percent M.A.C.)	Moment of inertia, I_Y (slug-ft^2)
11,600		27.3	28.5	27,283

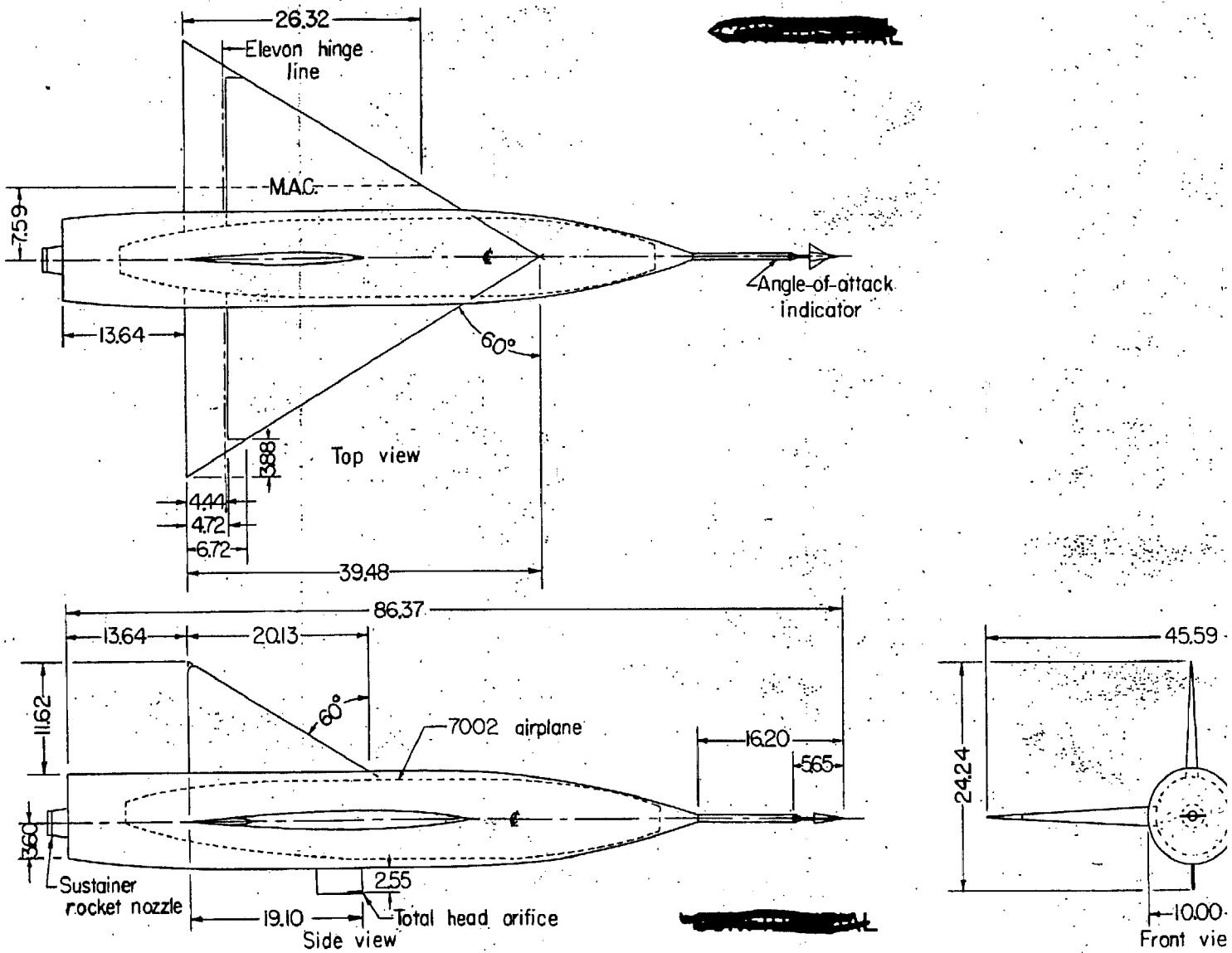

Figure 1.- Three-view drawing of the $\frac{1}{8}$-scale MX-813 rocket-powered flight model; all dimer in inches. Consolidated Vultee 7002 airplane is sketched in for comparison.

Figure 2.- Side view of one of the MX-813 models.

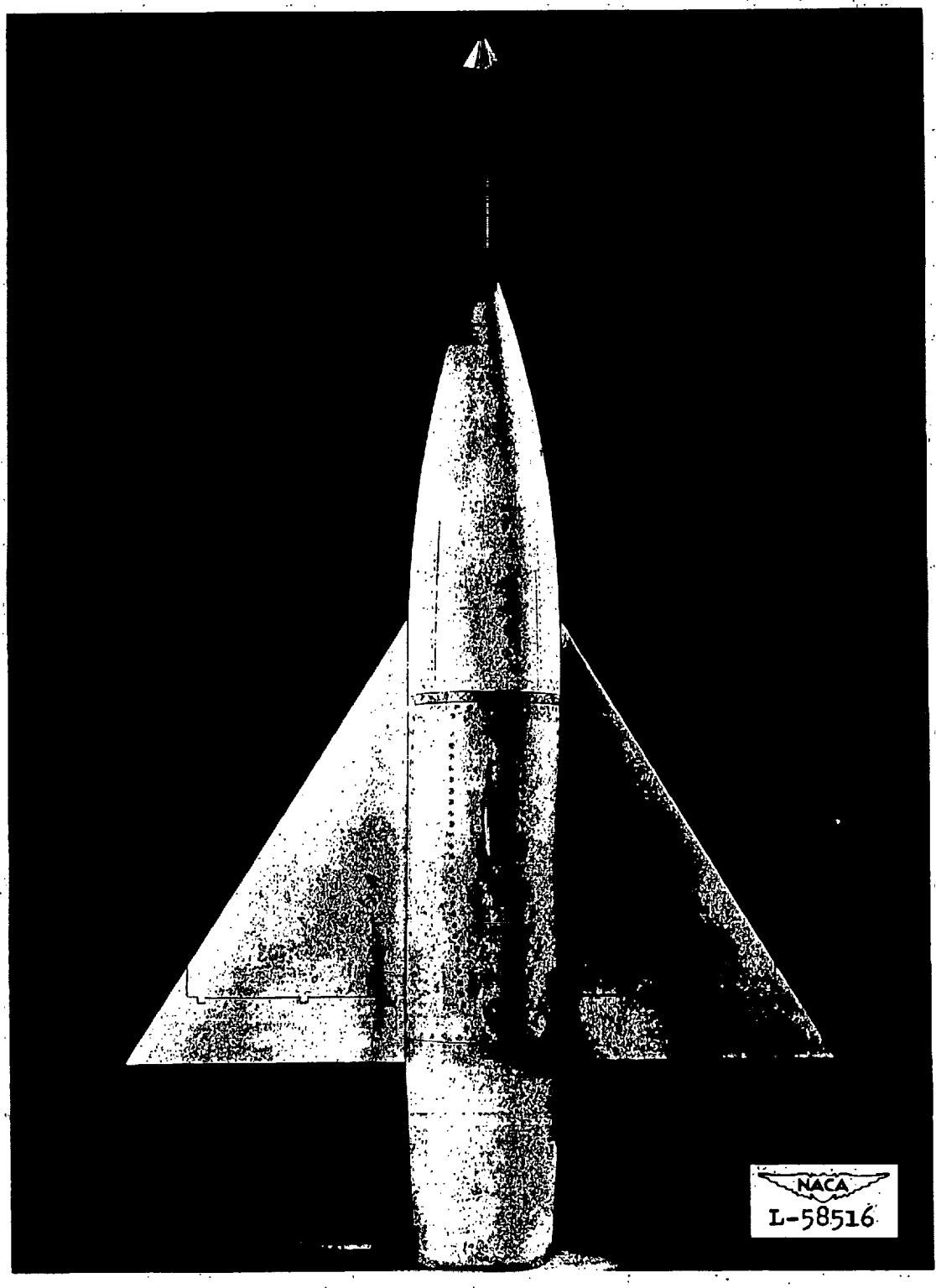

Figure 3.- Bottom view of one of the MX-813 models.

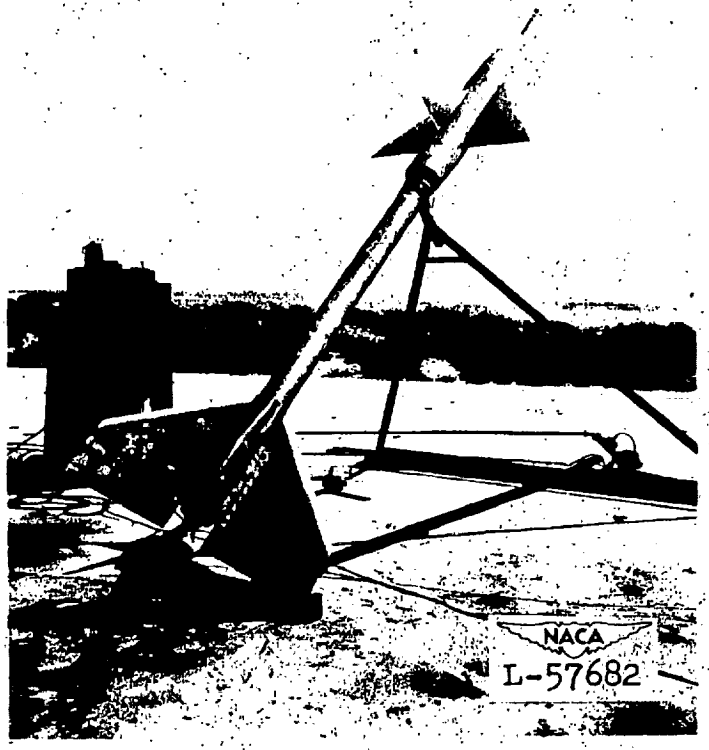

Figure 4.- MX-813 model-booster combination on launcher.

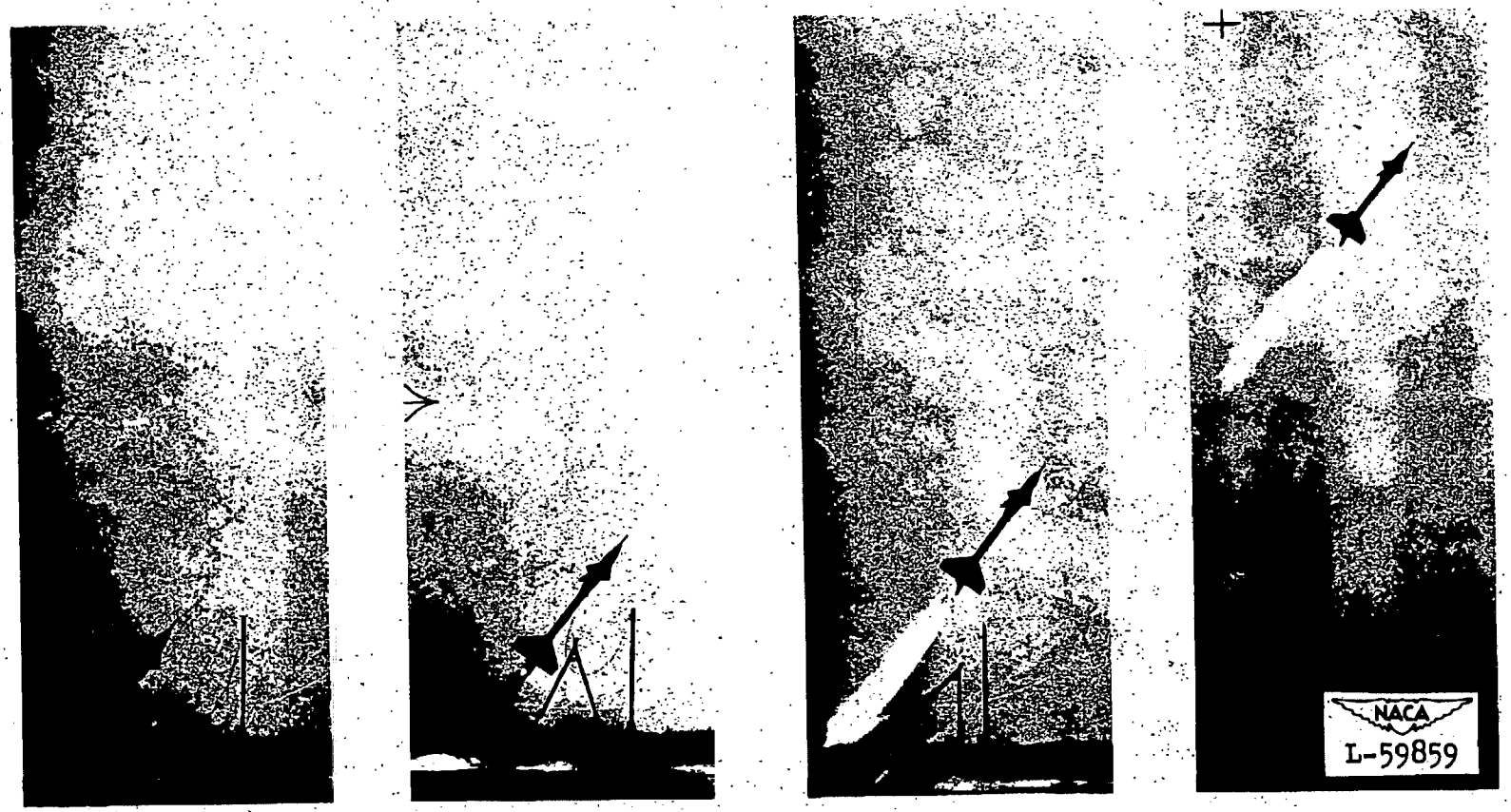

Figure 5.- Photographs of launching of $\frac{1}{8}$-scale model of the MX-813.

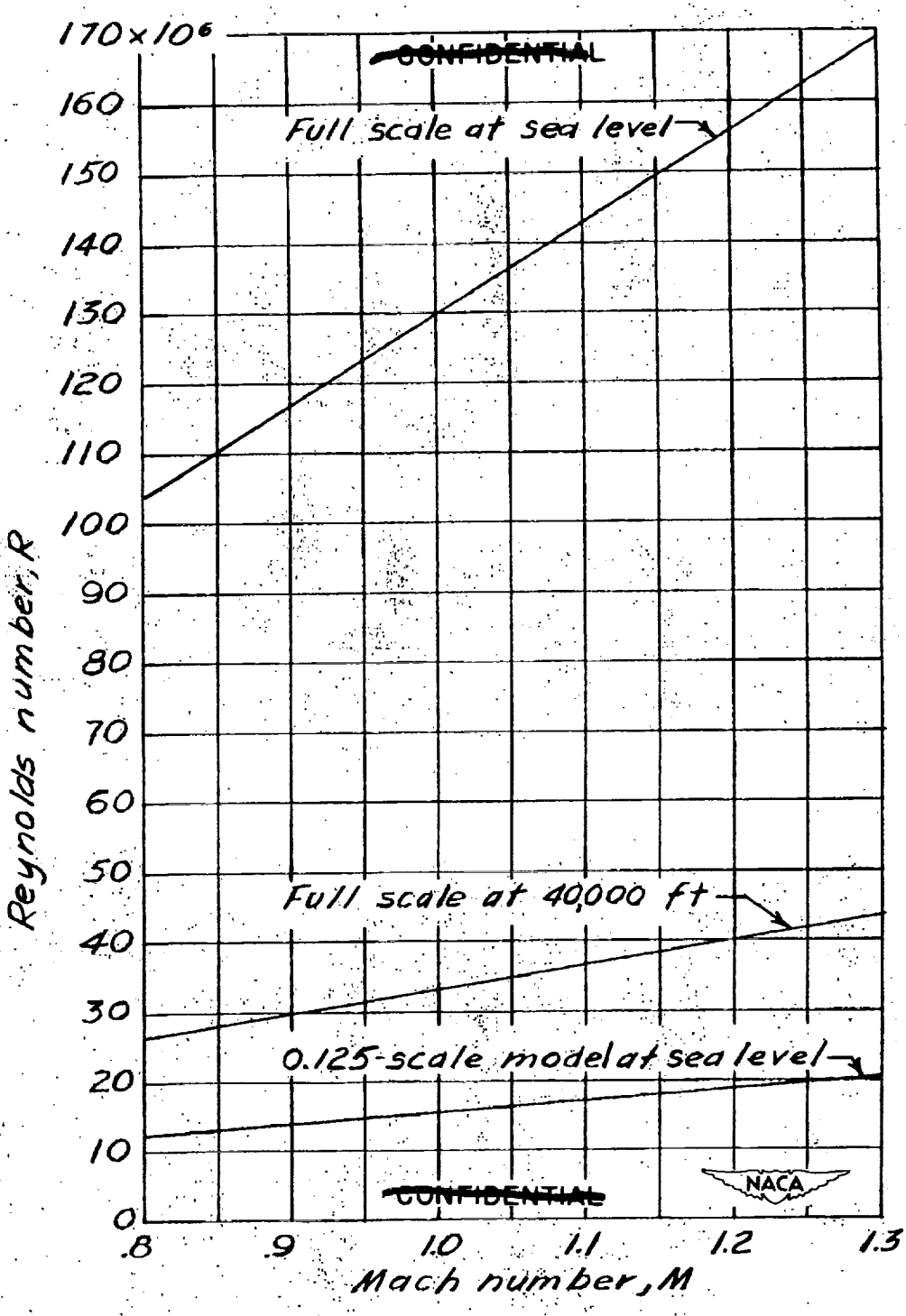

Figure 6.- Variation of Reynolds number with Mach number for flight of the MX-813 at two altitudes and for flight model test data.

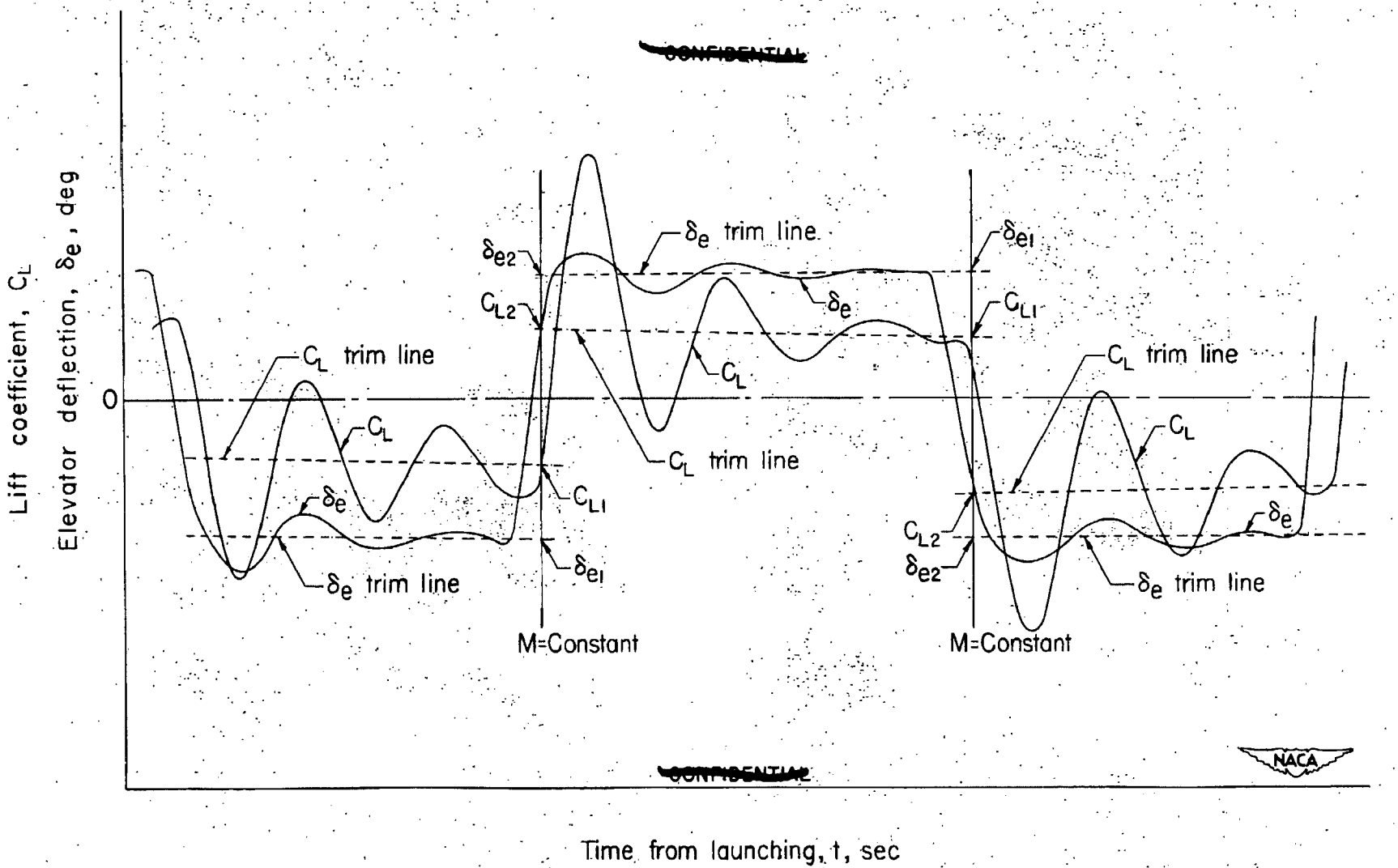

Figure 7.- Typical section of time history as used for data analysis.

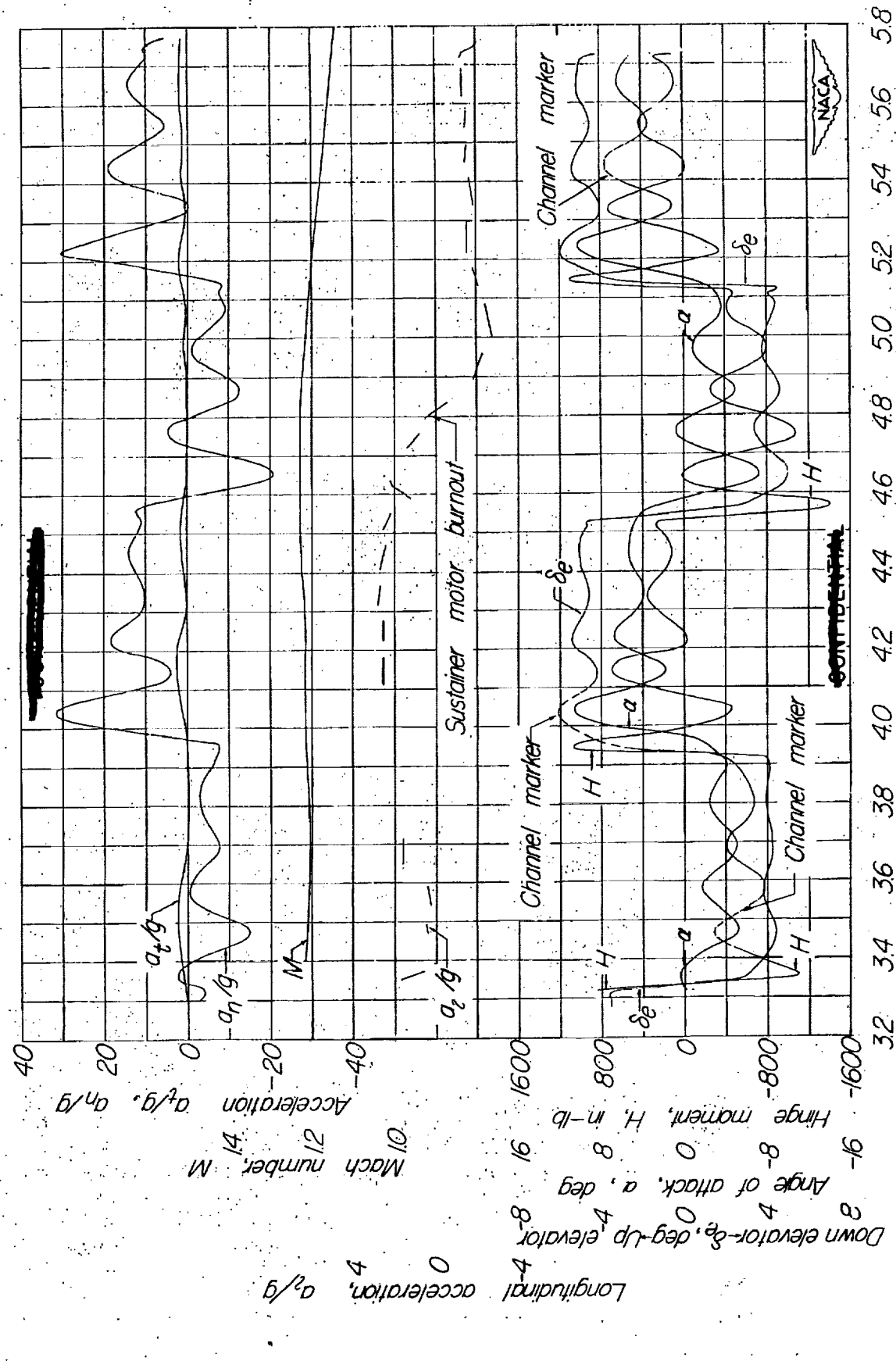

Figure 8.- Time history of flight of MX-813 model 1. Center of gravity at 0.25c.

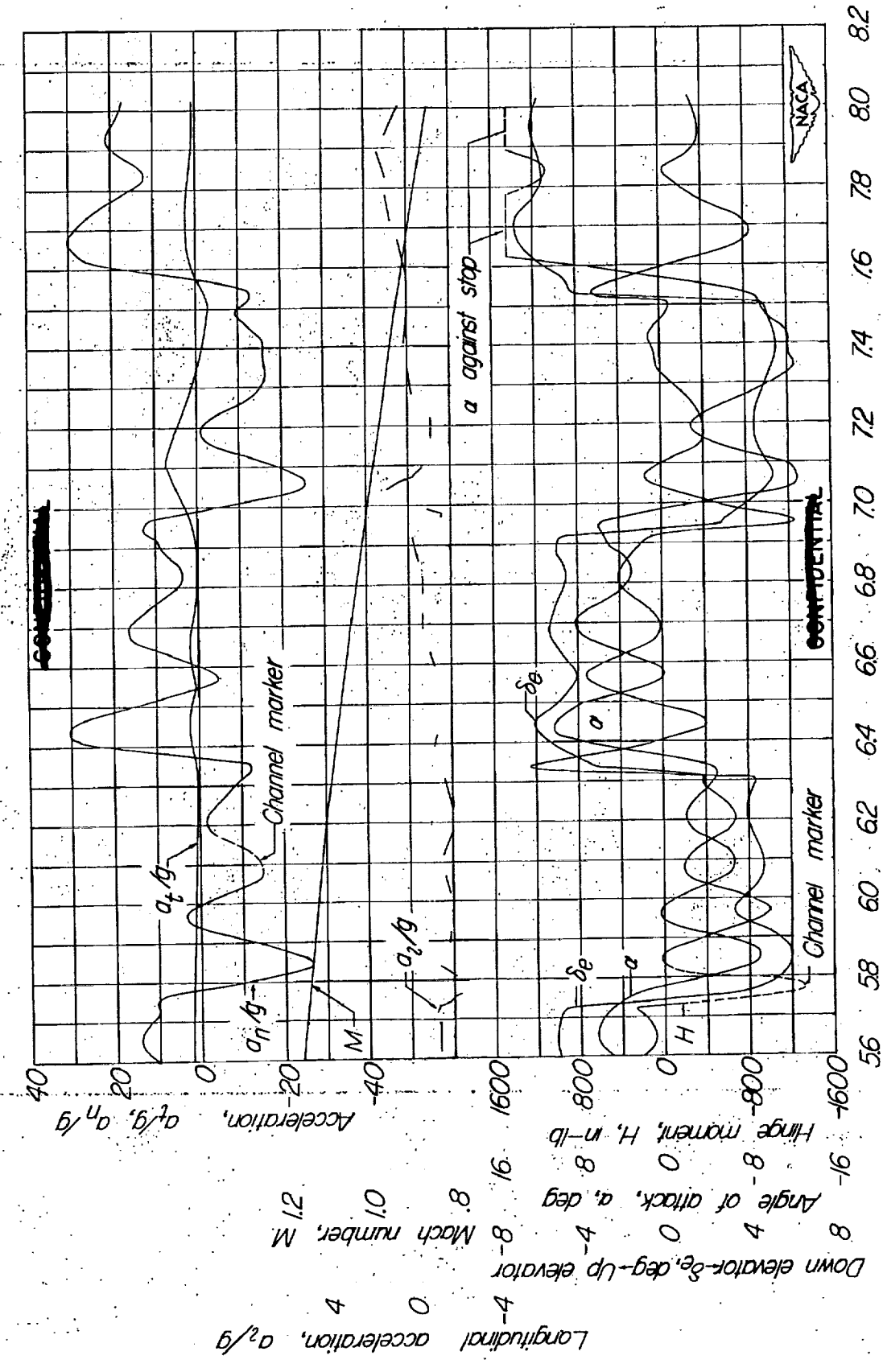

Figure 8.- Concluded.

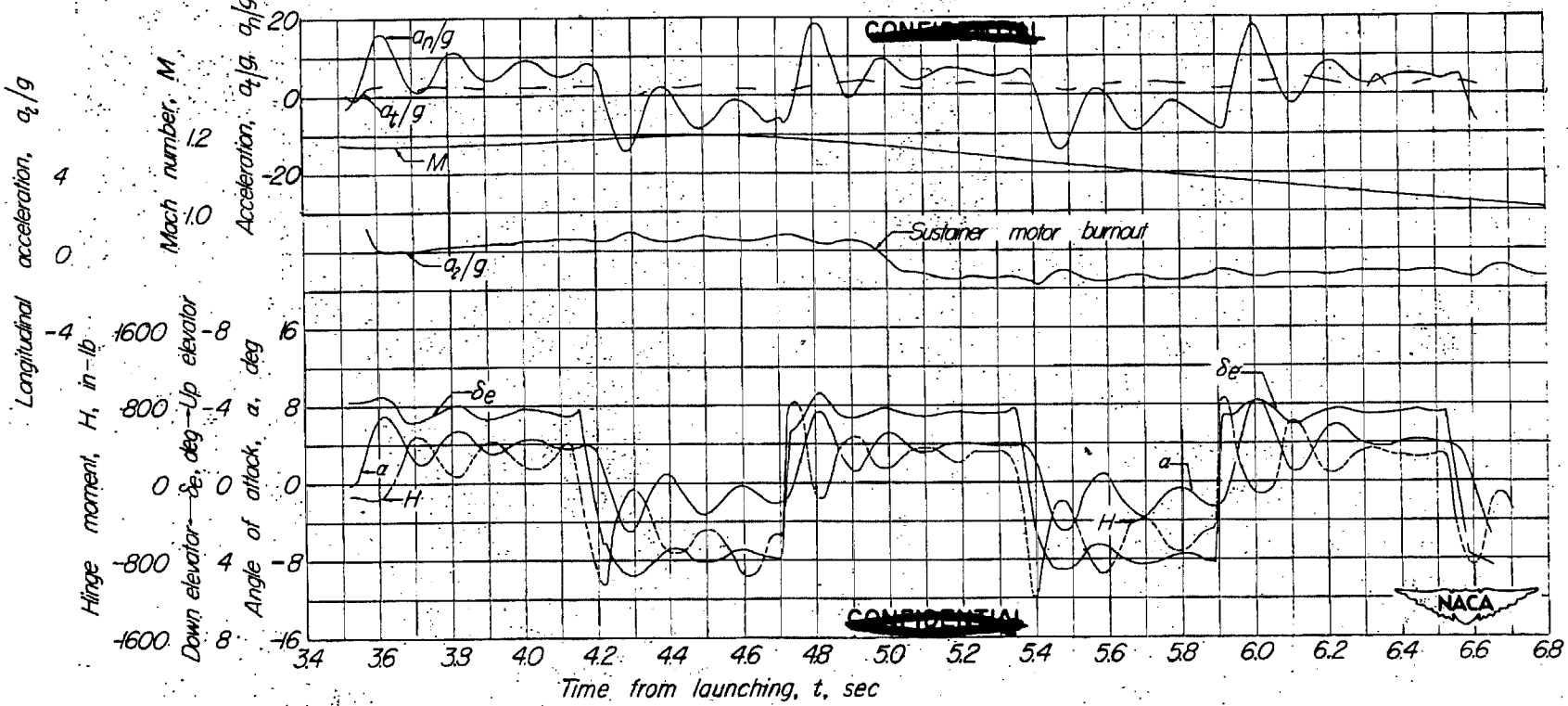

Figure 9.- Time history of the flight of MX-813 model 2. Center of gravity at 0.20$\bar{c}$.

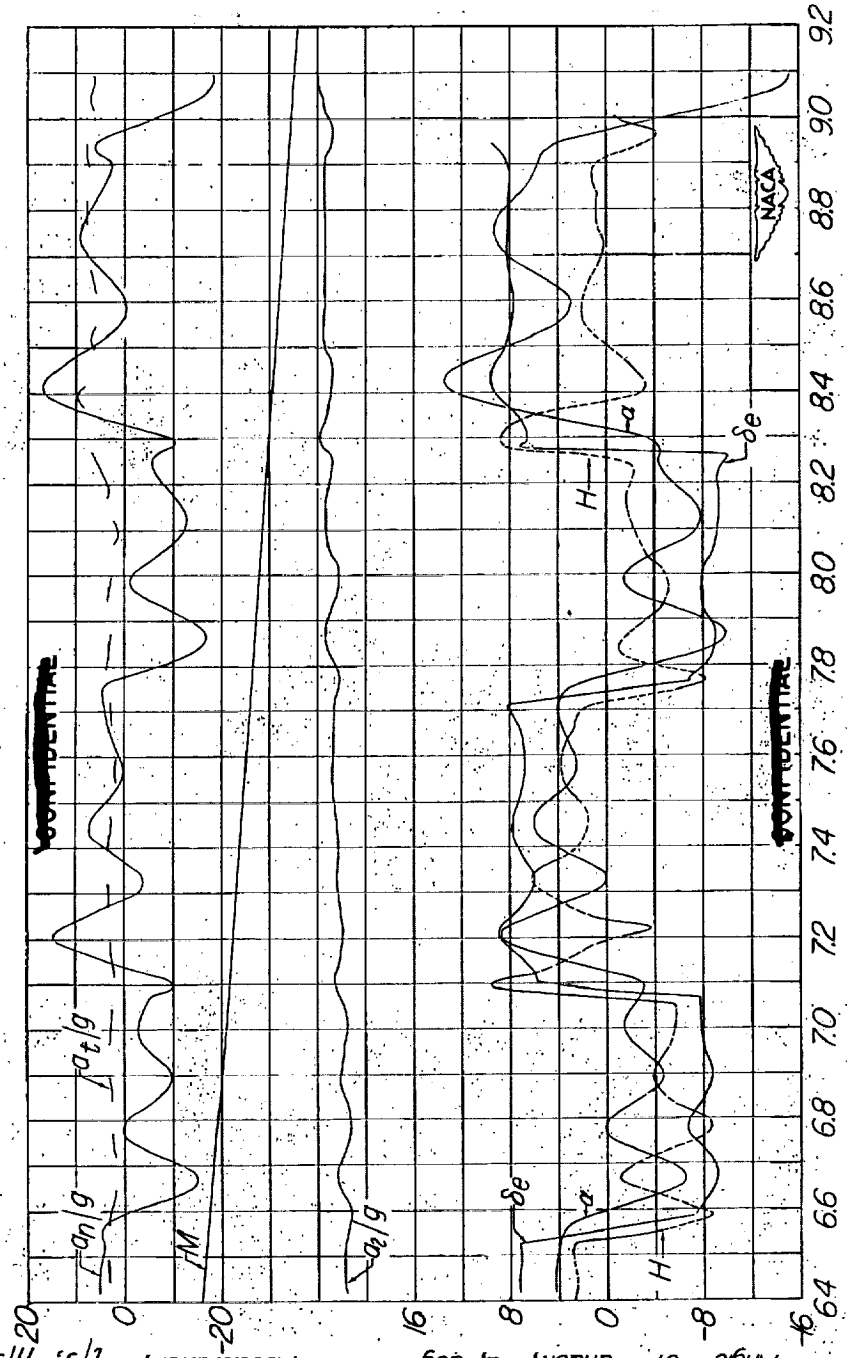

Figure 9.- Concluded.

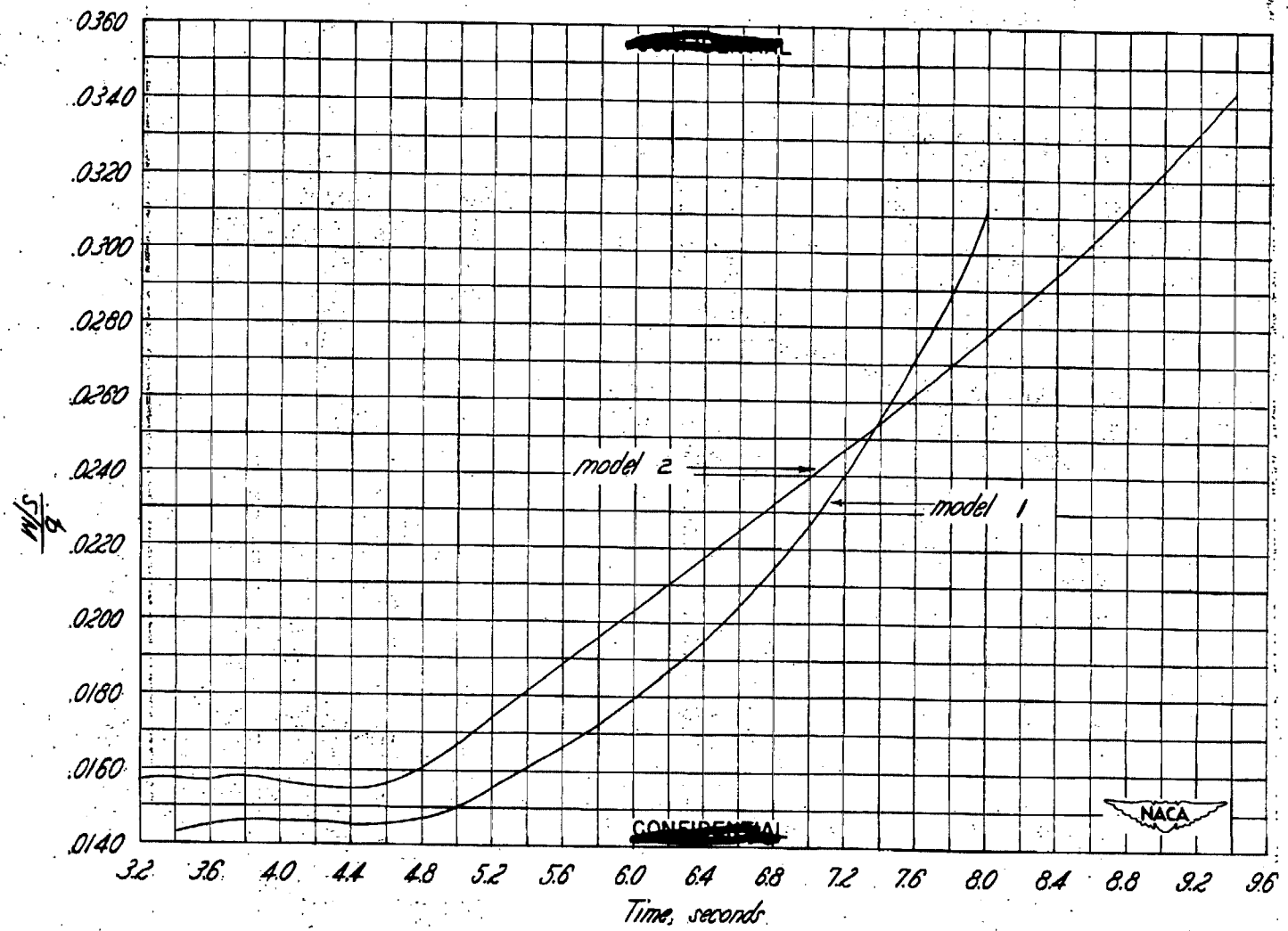

Figure 10.- Variation of $\frac{W/S}{q}$ with time for MX-813 models.

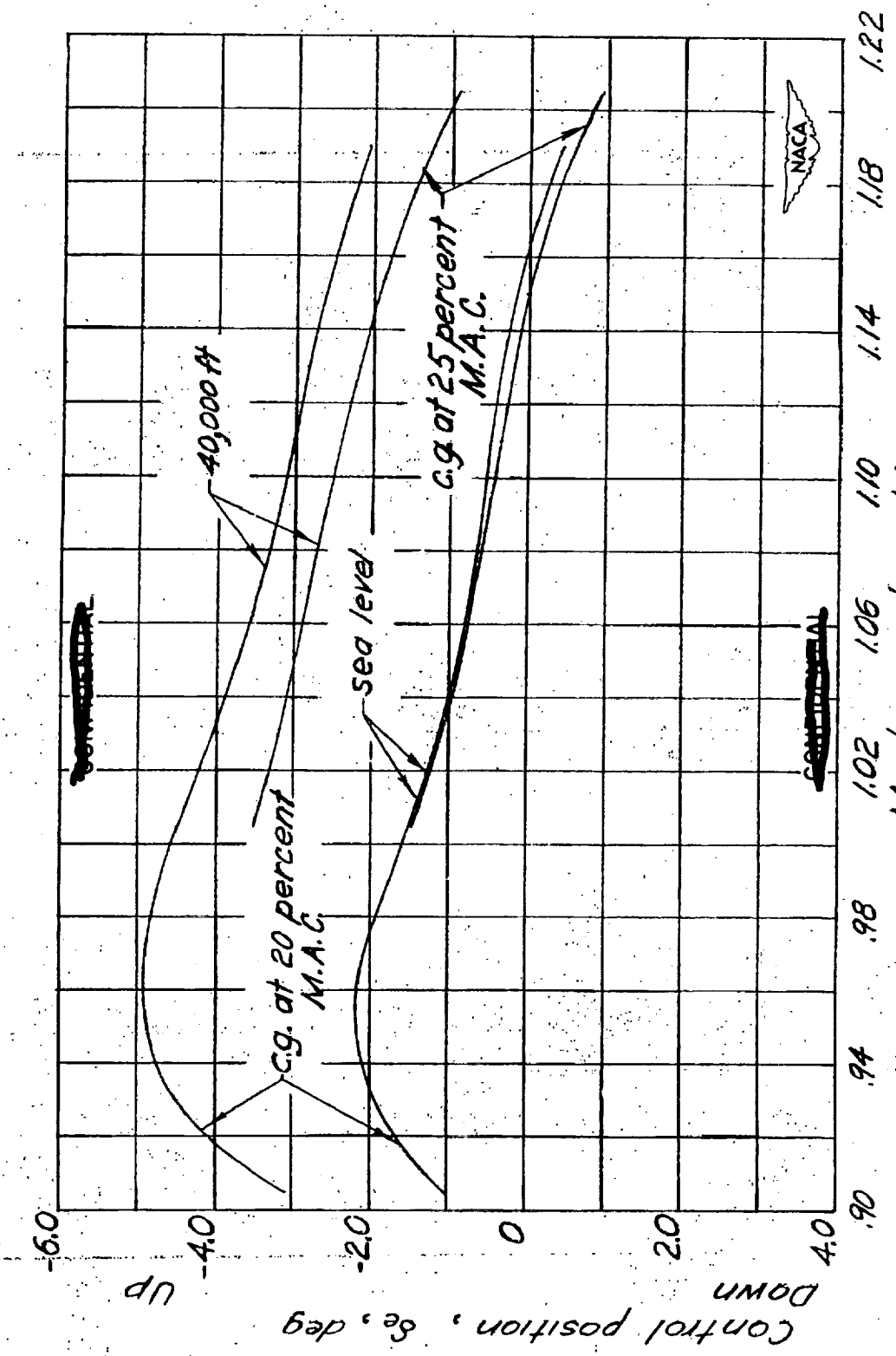

Figure 11.- Variation with Mach number of the control position required for trim in level flight at various altitudes and center-of-gravity locations.

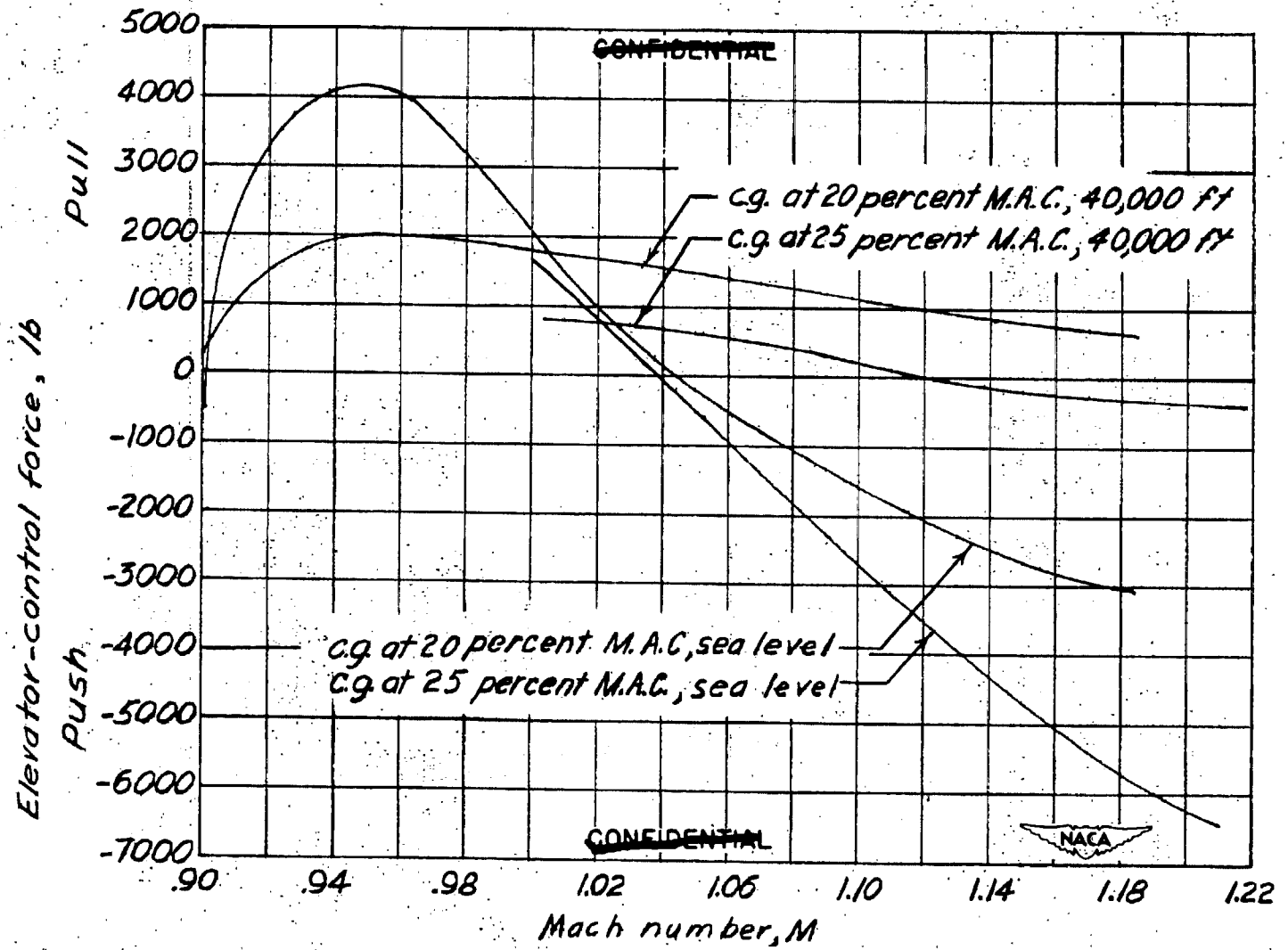

Figure 12.- Variation with Mach number of the elevator control force required for trim in level flight at different altitudes and center-of-gravity locations.

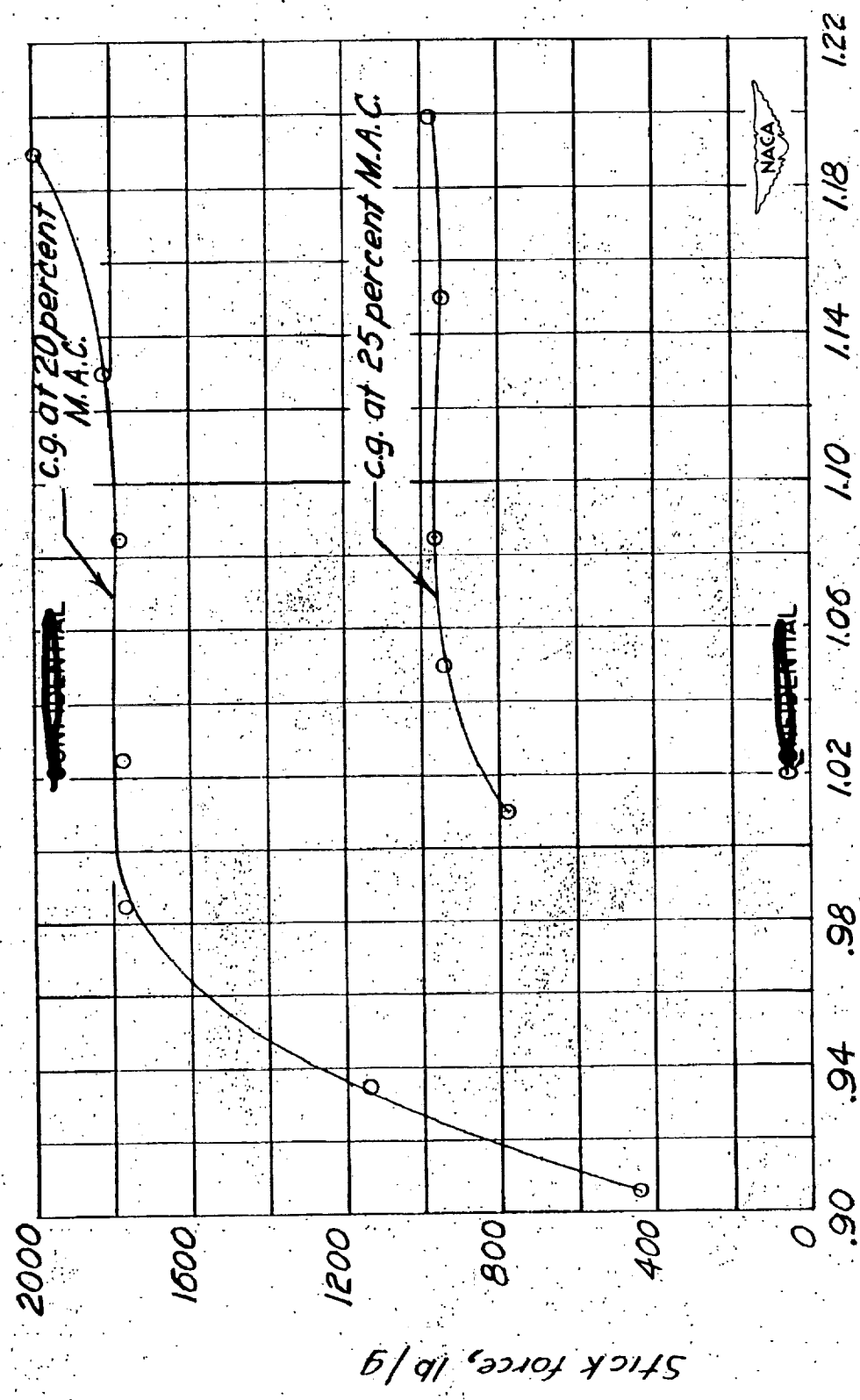

Figure 13.- Variation of stick force per g with Mach number for different center-of-gravity locations.

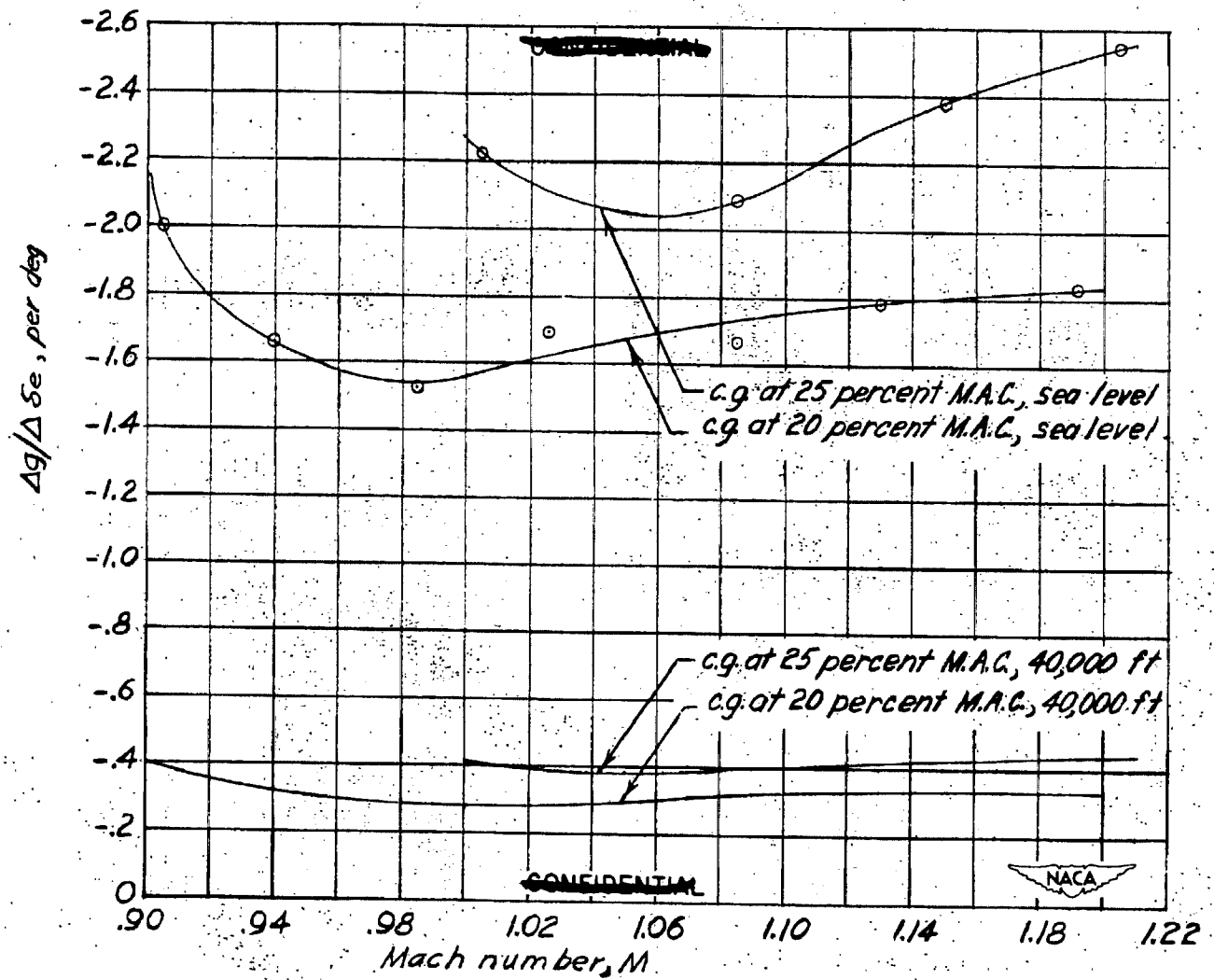

Figure 14.- Variation with Mach number of the normal acceleration produced per unit elevator deflection at different altitudes and center-of-gravity locations.

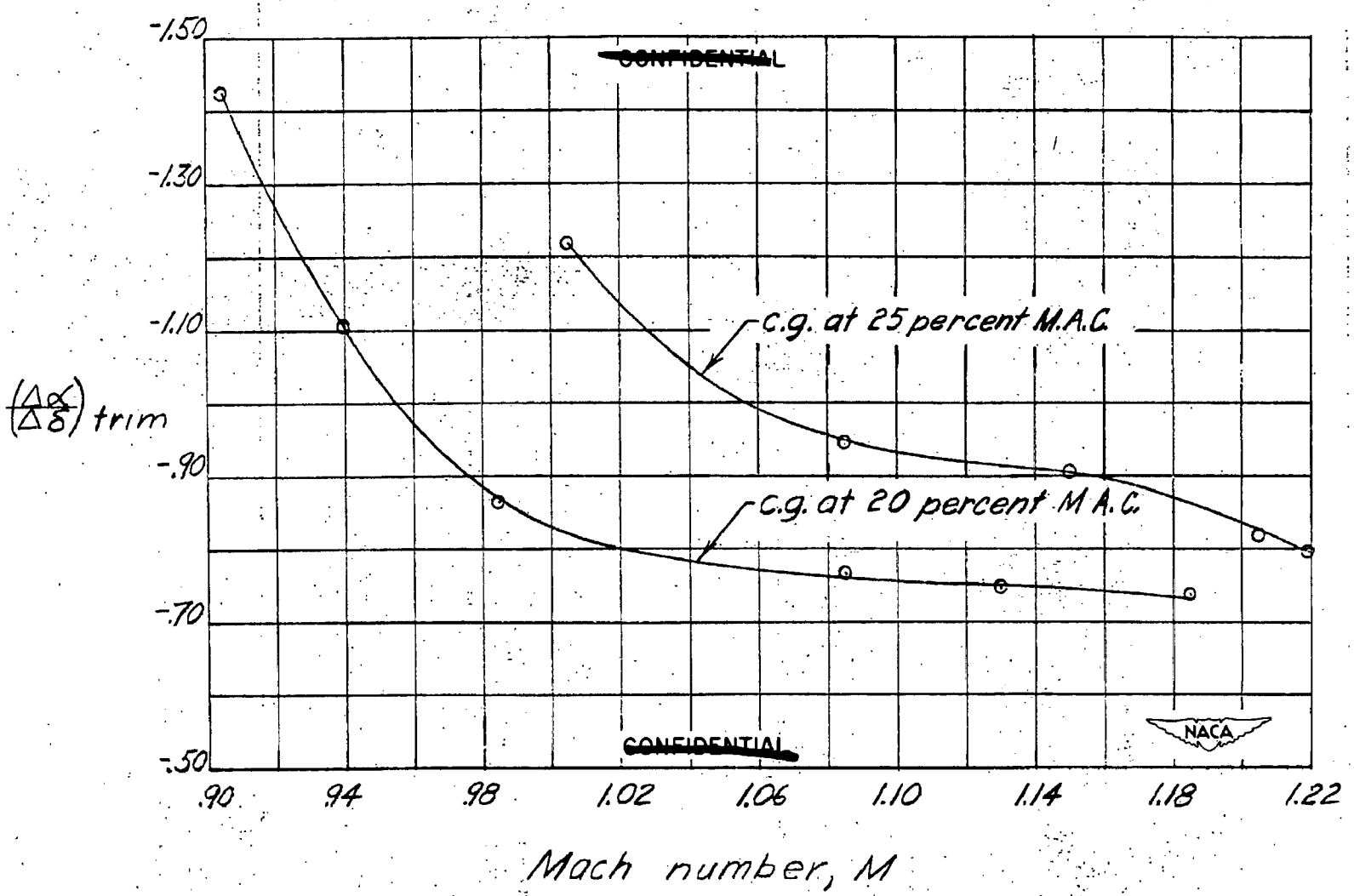

Figure 15.- Variation with Mach number of the angle-of-attack change produced per degree elevator deflection at different center-of-gravity locations.

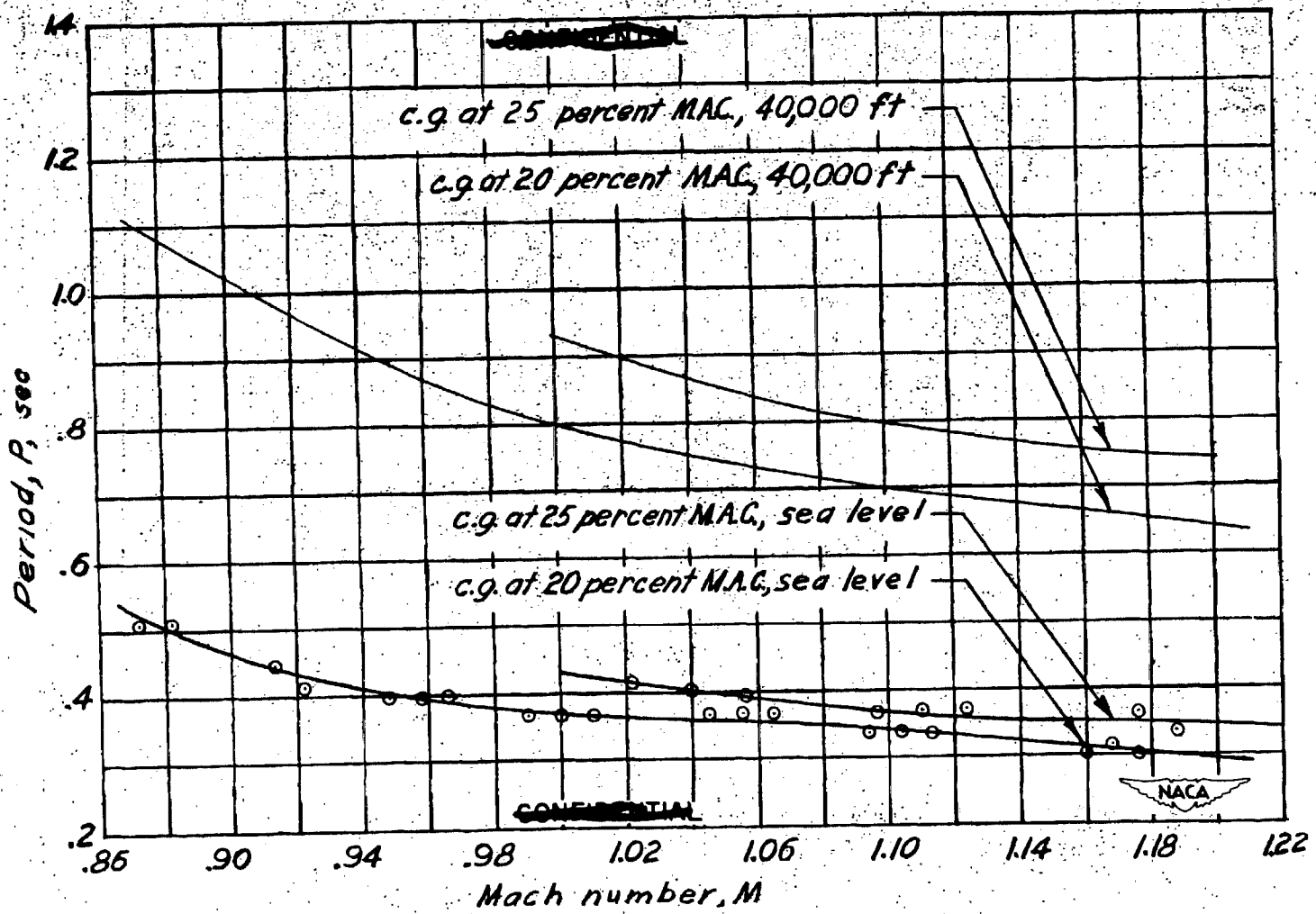

Figure 16.- Variation with Mach number of the period of the short-period longitudinal oscillation.

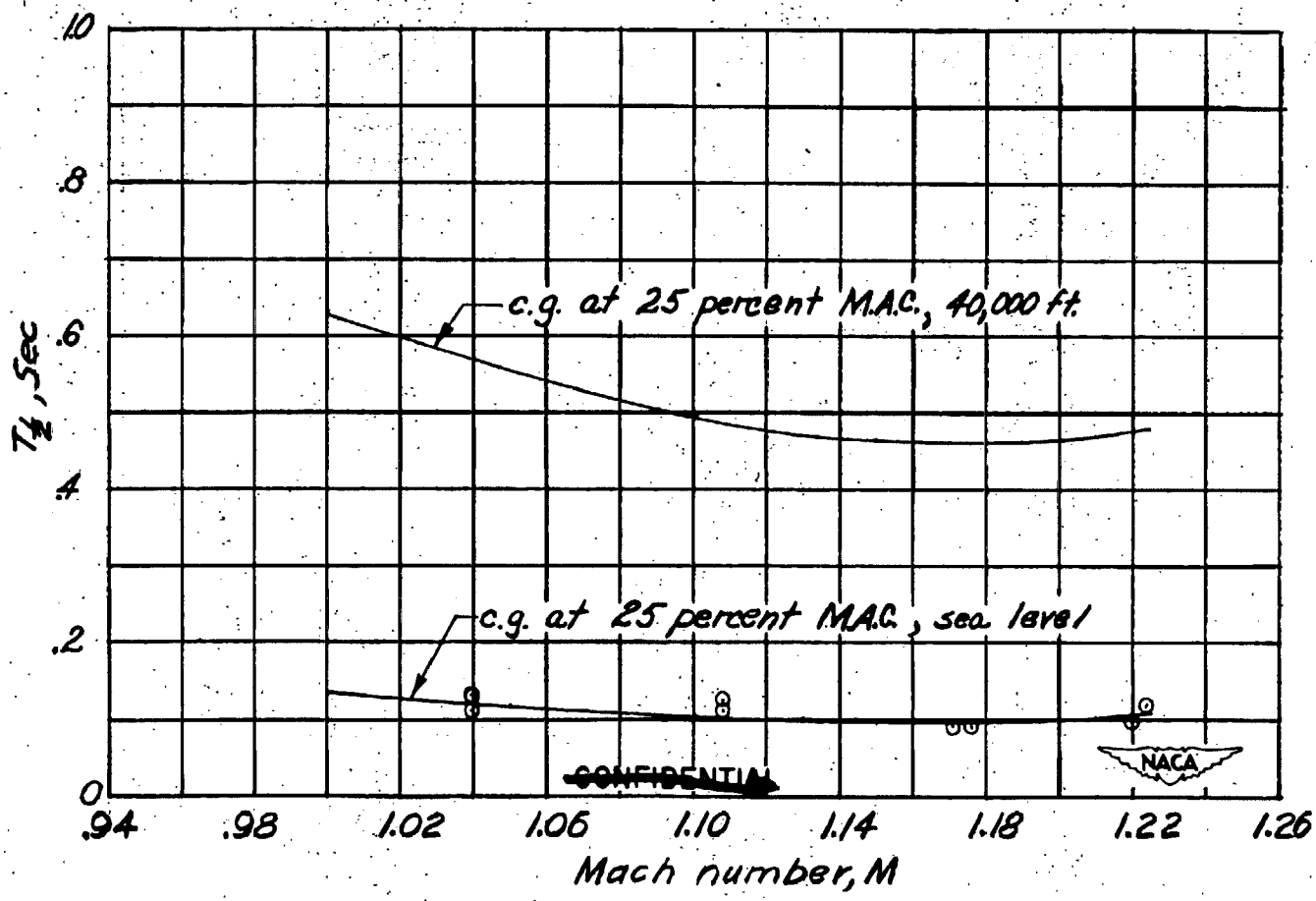

Figure 17.- Variation with Mach number of the time required for the short-period longitudinal oscillation to damp to one-half amplitude.

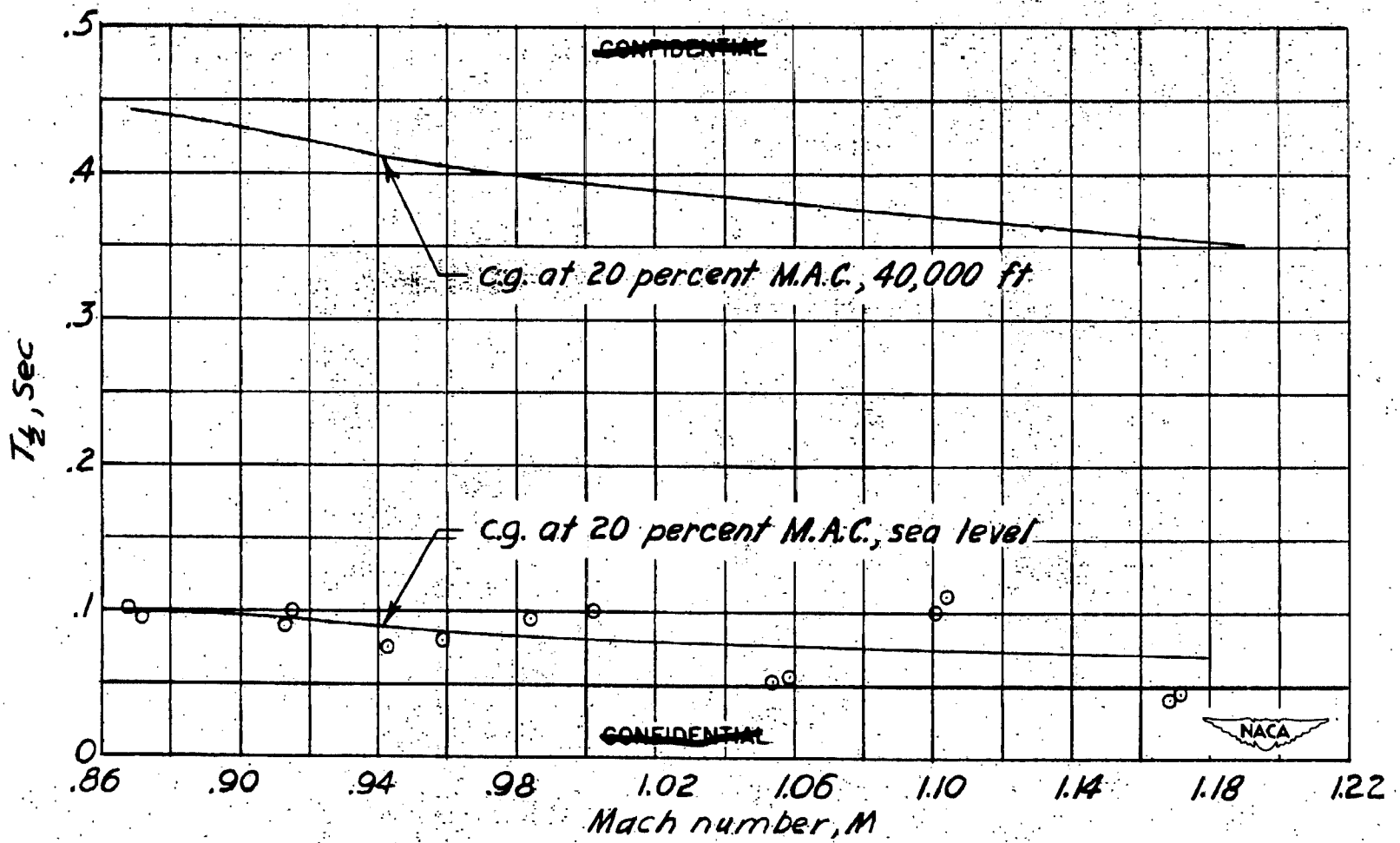

Figure 18.- Variation with Mach number of the time required for the short-period longitudinal oscillation to damp to one-half amplitude.